

Hole-depletion of ladders in $\text{Sr}_{14}\text{Cu}_{24}\text{O}_{41}$ induced by correlation effects

V. Ilakovac^{1,2,*}, C. Gougoussis³, M. Calandra³, N. B. Brookes⁴, V. Bisogni⁴, S. G. Chiuzbaian¹, J. Akimitsu⁵, O. Milat⁶, S. Tomić⁶, and C. F. Hauge^{1*}

¹Laboratoire de Chimie Physique Matière et Rayonnement, UPMC, CNRS, F-75231 Paris, France

²Université de Cergy-Pontoise, F-95031 Cergy-Pontoise, France

³Institut de Minéralogie et de Physique des Milieux Condensés, UPMC, CNRS, F-75252, Paris, France

⁴ESRF, B.P. 220, 38043 Grenoble Cedex, France

⁵Department of Physics, Aoyama-Gakuin University, Setagaya, Tokyo 157-8572, Japan

⁶Institut za fiziku, P.O. Box, HR-10001 Zagreb, Croatia

(Dated: January 16, 2021)

The hole distribution in $\text{Sr}_{14}\text{Cu}_{24}\text{O}_{41}$ is studied by low temperature polarization dependent O K Near-Edge X-ray Absorption Fine Structure measurements and state of the art electronic structure calculations that include core-hole and correlation effects in a mean-field approach. Contrary to all previous analysis, based on semi-empirical models, we show that correlations and antiferromagnetic ordering favor the strong chain hole-attraction. For the remaining small number of holes accommodated on ladders, leg-sites are preferred to rung-sites. The small hole affinity of rung-sites explains naturally the 1D - 2D cross-over in the phase diagram of $(\text{La},\text{Y},\text{Sr},\text{Ca})_{14}\text{Cu}_{24}\text{O}_{41}$.

PACS numbers: 78.70.Dm, 71.15.Mb, 74.78.-w, 74.72.Gh

I. INTRODUCTION

The quasi-one-dimensional spin chain and ladder $(\text{La},\text{Y},\text{Sr},\text{Ca})_{14}\text{Cu}_{24}\text{O}_{41}$ compounds have attracted considerable interest since the discovery of a quantum critical phase transition in their phase diagram.¹ These compounds are the first superconducting copper oxide materials with a non-square lattice. They are composed of alternately stacked chain and ladder planes. The chains are made up of CuO_2 linear edge-sharing CuO_4 squares and the ladder planes consist of two zig-zag strings of corner-sharing Cu_2O_3 squares (see Fig. 1). The parent compound $\text{Sr}_{14}\text{Cu}_{24}\text{O}_{41}$ is naturally doped with six holes per formula unit (*fu*).

Determining exactly how the holes are distributed in the system is hindered by the complexity of the crystal structure of $\text{Sr}_{14}\text{Cu}_{24}\text{O}_{41}$ and electron correlation effects.^{2,3} Room temperature optical conductivity,⁴ Near-Edge X-ray Absorption Fine Structure (NEXAFS),⁵ X-ray emission spectroscopy,⁶ and Hall coefficient measurements⁷ on $\text{Sr}_{14}\text{Cu}_{24}\text{O}_{41}$ estimated that at least *five* holes per *fu* reside in chains and at most *one* in ladders. High density of holes in chains is compatible with the low temperature $T_C \approx 200$ K⁸ charge ordering with the 5-fold *chain* periodicity accompanying the antiferromagnetic (AF) spin-dimerization, observed by inelastic neutron scattering.⁹⁻¹¹ In ladders, a gapped spin-liquid and the charge density wave (CDW) appear in the ground state, in the spin and charge sectors, respectively. Whereas the spin-liquid and its collective spin excitations (triplons) are well understood theoretically and experimentally,¹²⁻¹⁴ the low hole density in the charge sector is at variance with the 5-fold periodicity in *ladder* cell units (Wigner hole crystal) observed by low temperature resonant X-ray diffraction measurements at the O K edge if a $4k_F$ CDW picture is assumed.¹⁵ On the other hand, a revisited interpretation of NEXAFS spectra¹⁶

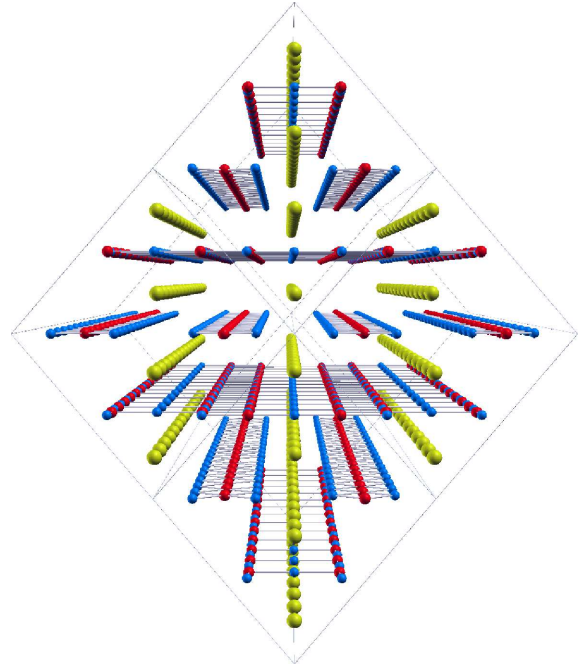


FIG. 1: (Color online) 3D view along the *c* crystal axis of four 316-atom AF unit cells of $\text{Sr}_{14}\text{Cu}_{24}\text{O}_{41}$. The structure is composed of alternately stacked *chain* layers, constituted of CuO_2 linear edge-sharing CuO_4 squares, and *ladder* planes, made up of two zig-zag strings of Cu_2O_3 corner-sharing squares. They are parallel to the (\mathbf{a},\mathbf{c}) -plane and separated by Sr atoms. Cu/O/Sr atoms are colored in red/blue/yellow.

claimed a distribution of 2.8 holes in ladders and 3.2 holes in chains, which satisfactorily explains the CDW in ladders, while it fails to explain AF dimer order in chains.

The apparently contradictory results are mainly re-

lated to the lack of a suitable theoretical model. All published NEXAFS analyses are based on semi-empirical models that do not take explicitly into account the complex interplay between spins and holes in ladders and chains. Thus the basic question of where the holes reside in $\text{Sr}_{14}\text{Cu}_{24}\text{O}_{41}$ has remained unresolved up to now.

The hole distribution between chains and ladders is the key to stabilization of interdependent electronic phases in these two subsystems. It is a prerequisite to understanding the low-energy physics of the system and such open issues as the occurrence of Zhang-Rice singlets,¹⁷ the evolution of spin order and the origin of the superconductivity in the Ca-doped compound.² We bridge the gap between theory and experiment by performing low temperature electron yield polarization dependent O K pre-edge NEXAFS measurements and state-of-the-art electronic structure calculations. In the theoretical modeling we consider the full 316-atom AF unit cell, include the core-hole effects, core level shift and correlations in a DFT+U framework. This method has proven to be fairly successful in reproducing X absorption spectra in correlated metals with well localized orbitals^{19,23}. We show that, contrary to previous claims, correlation effects and AF order stabilize holes on chains, induce hole-depletion in ladders, where rung sites become less populated than leg sites.

II. EXPERIMENTAL AND CALCULATION DETAILS

High-quality single crystals of $\text{Sr}_{14}\text{Cu}_{24}\text{O}_{41}$ were grown by the traveling-solvent floating-zone method and characterized by X-ray diffraction measurements. A well oriented sample was cleaved *in-situ* along the (a,c) plane under a pressure of 10^{-10} mbar. The O K edge NEXAFS measurements were performed using the helical undulator Dragon beam line ID08 at the European Synchrotron Radiation Facility (ESRF) in the total electron yield mode with 200 meV resolution. The incident light was normal to the sample surface and its polarization was parallel to the a/c sample axis.

NEXAFS calculations are performed by the XSPECTRA¹⁸⁻²⁰ code based on Density Functional Theory (DFT)²¹ and all-electron wave function reconstruction.²² Correlation effects are simulated in a mean field DFT+U framework^{23,24} using a Hubbard on-site energy of $U_{dd} = 10$ eV for copper and $U_{pp} = 4$ eV for oxygen. The chain and ladder atomic positions were taken from Gotoh et al.²⁵ without imposing any superstructure modulations, either along the chains or along the ladders. We performed a specific NEXAFS calculation for *each* of the five inequivalent oxygen sites existing in the structure, two in the ladders, and three in the chains. We find a negligible core-level-shift.

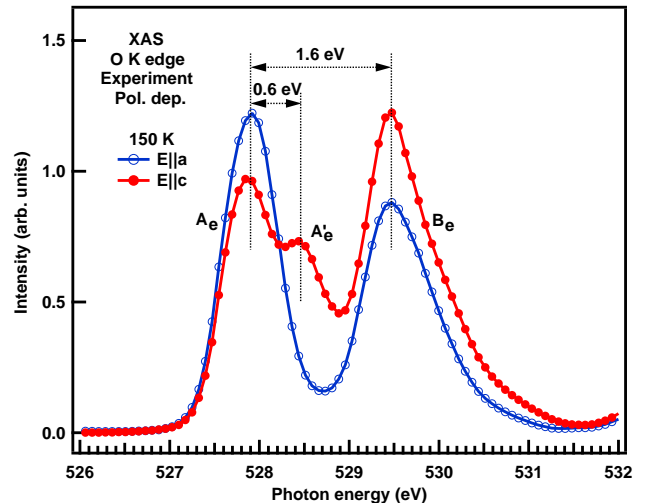


FIG. 2: (Color online) Polarization dependent O K NEXAFS pre-edge intensity for $\mathbf{E}||\mathbf{a}$ and $\mathbf{E}||\mathbf{c}$ measured at 150 K. Subscript e is for experiment.

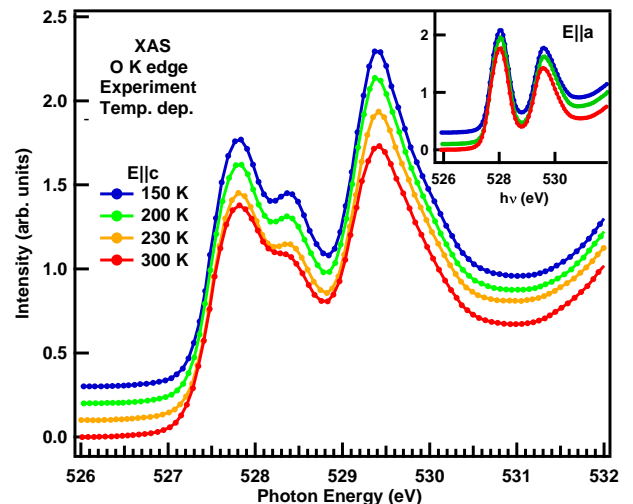


FIG. 3: (Color online) Temperature dependence of the O K NEXAFS pre-edge intensity for $\mathbf{E}||\mathbf{c}$ showing that for this polarization spectra change below and above the charge ordering temperature (≈ 200 K). The inset shows that the $\mathbf{E}||\mathbf{a}$ spectra temperature change is negligible.

III. RESULTS AND DISCUSSION

A. NEXAFS measurements

The low temperature (150 K, see Fig. 2) O K NEXAFS pre-edge spectra has two distinct structures, A_e , centered at 527.9 eV and B_e , at 529.5 eV (e is for “experiment”), in agreement with previously published room-temperature spectra.^{5,6,16} The shape of the two structures is depen-

dent on the polarization of the incident photon: for $\mathbf{E}\parallel\mathbf{a}$, A_e is stronger than B_e , while for $\mathbf{E}\parallel\mathbf{c}$ (direction along the chains and the ladders) it is the opposite. For $\mathbf{E}\parallel\mathbf{c}$ structure A_e has a second, well resolved peak at 528.5 eV, A'_e . The intensity of this structure is only weakly affected by the charge ordering transition (see Fig. 3). The $\mathbf{E}\parallel\mathbf{a}$ spectra are even less affected at T_C (see Fig. 3 inset). The attribution of the features in these spectra has so far been very controversial.^{5,15,16}

B. Calculation of the NEXAFS spectra

Theoretical modeling using the AF unit cell with 5-fold periodicity in chains is shown in Fig. 4. The two, A_e and B_e , structures are well reproduced in the calculations (labeled A_c and B_c where c is for the calculated spectra), although their separation is only 0.7 eV, compared to 1.6 eV for the experiment. This discrepancy is attributed to the well-known underestimation of the Hubbard gap in DFT+U simulations. The agreement between theory and experiment is particularly good for the $\mathbf{E}\parallel\mathbf{c}$ polarization as in the c -direction the charges are less localized. For $\mathbf{E}\parallel\mathbf{c}$ (i) the B_c cross section is stronger than the A_c cross section, and (ii) the high-energy shoulder A'_c is clearly visible. For $\mathbf{E}\parallel\mathbf{a}$ polarization, the B_c structure has smaller cross section than the A_c peak.

The two insets in Fig. 4 show the calculated cross section contribution of chain (C), ladder-leg (L) and ladder-rung (R) oxygens to the NEXAFS spectra. The contribution from ladder-rungs is small or negligible for all features except for the B_c peak in the $\mathbf{E}\parallel\mathbf{a}$ geometry. This result is in line with the analysis by Nücker et al.⁵ and is in strong disagreement with the results of Rusydi et al.¹⁶ where the contribution of ladder rungs was overestimated. Our results demonstrate that *ladder-rungs are hole-depleted in $\text{Sr}_{14}\text{Cu}_{24}\text{O}_{41}$* .

For both polarizations the low energy A_c peak is equally composed of chain and ladder-leg states, with a minor contribution from ladder-rungs in the $\mathbf{E}\parallel\mathbf{a}$ geometry. Its high energy A'_c shoulder is composed of both ladder-leg and *chain* contributions. This result is in stark disagreement with all previous claims based on semi-empirical NEXAFS analysis^{5,16} that attribute the A'_c structure solely to ladders. It points to the fact that the O K edge resonant diffraction results, performed at the photon energy corresponding to A'_c , could be related to the modulation reflections due to the chain-ladder lattice mismatch²⁶. The Wigner-hole crystallization analysis of the O K edge resonant soft X-ray scattering data in Ref. 15 now becomes questionable.

Calculations using the AF unit cell with 4-fold periodicity in chains²⁷ is shown in Fig. 5. The two insets show the calculated cross section contribution of chain (C), ladder-leg (L) and ladder-rung (R) oxygens, equivalent to these in Fig. 4. The experimental results are less well reproduced compared to the 5-fold chain-periodicity unit cell. First, the $A_c - B_c$ energy separation is smaller. Fur-

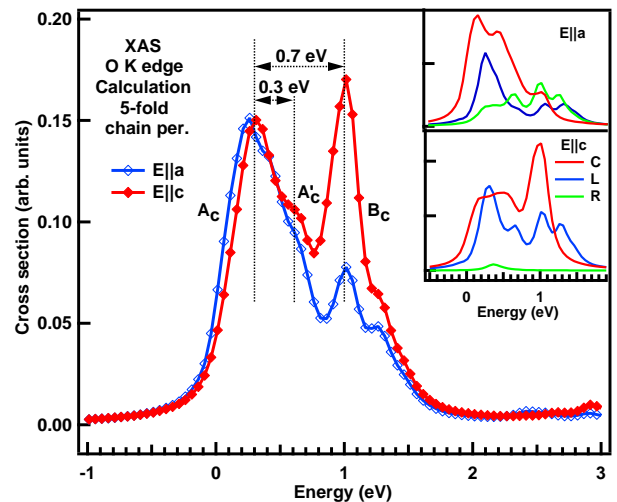


FIG. 4: (Color online) Calculated O K NEXAFS pre-edge cross section on the AF unit cell with 5 fold periodicity in chains, for $\mathbf{E}\parallel\mathbf{a}$ and $\mathbf{E}\parallel\mathbf{c}$. Insets : contribution of chain (C), ladder-leg (L) and ladder-rung (R) oxygens for $\mathbf{E}\parallel\mathbf{a}$ (upper inset) and $\mathbf{E}\parallel\mathbf{c}$ (lower inset). Zero energy corresponds to a photon energy of 527.4 eV. Subscript c stands for calculated.

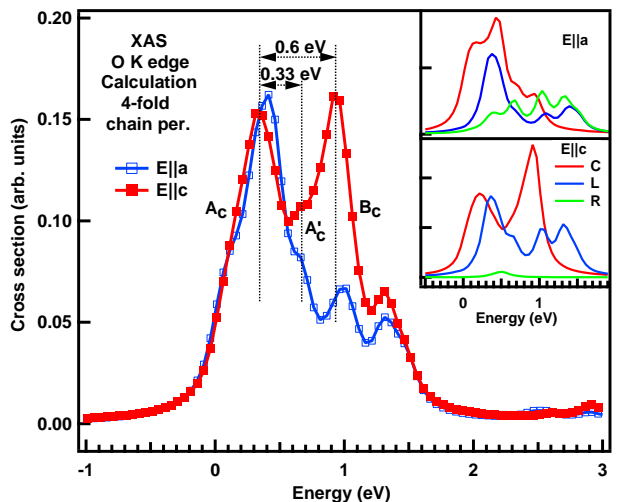


FIG. 5: (Color online) Calculated O K NEXAFS pre-edge cross section on the AF unit cell with 4 fold periodicity in chains, for $\mathbf{E}\parallel\mathbf{a}$ and $\mathbf{E}\parallel\mathbf{c}$. Insets : contribution of chain (C), ladder-leg (L) and ladder-rung (R) oxygens for $\mathbf{E}\parallel\mathbf{a}$ (upper inset) and $\mathbf{E}\parallel\mathbf{c}$ (lower inset). Zero energy corresponds to a photon energy of 527.4 eV.

ther, for the $\mathbf{E}\parallel\mathbf{c}$ geometry A_c and B_c are almost equal in intensity, contrary to the experiment. Finally, A'_c appears as a low energy shoulder to structure B_c and not as a high energy shoulder to A_c . For these reasons, the 4-fold chain-periodicity unit cell can be eliminated as a

model for chain spin ordering.

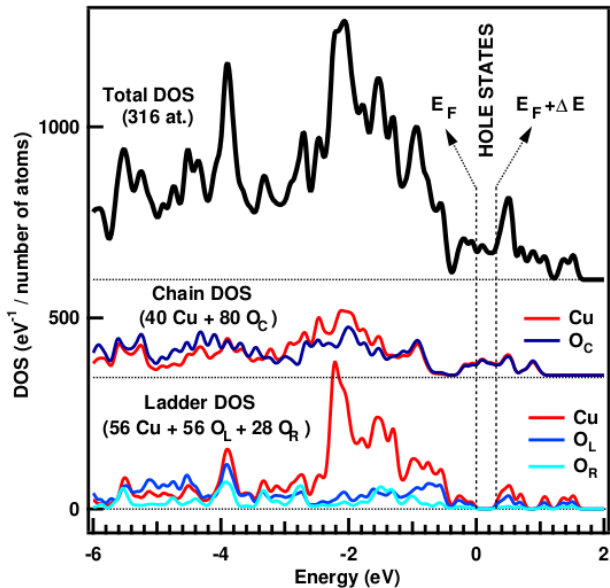


FIG. 6: (Color online) (upper panel) Total DOS of $\text{Sr}_{14}\text{Cu}_{24}\text{O}_{41}$ without a core-hole, calculated on the AF unit cell with 5 fold chain periodicity. The Fermi level (E_F) corresponds to 0 eV. (lower panels) Local chain- and ladder-DOS projected to Cu (red line) and O (blue lines). The second dotted line indicates where E_F would be if the system had 6 additional electrons per fu , i.e. no holes ($E_F' = E_F + \Delta E$, where $\Delta E = 0.31$ eV corresponds to additional $6 \times 4 = 24$ electrons).

C. Density of states

To understand the role of core-hole effects we also performed density of states (DOS) calculations for the system without a core-hole (see Fig. 4). Contrary to previous theoretical works,^{28–30} performed on a minimal cell without AF ordering, we find the occurrence of a 0.25 eV gap appearing in ladder states. This finding is in agreement with the insulating behavior of the ladders^{31–33} and points out the need of including the full AF crystal structure in the simulation. The occurrence of a 0.25 eV Hubbard gap in ladder states results in a strong hole depletion of this sub-system. Indeed, we find that only about 0.4 holes reside in ladders, while the chains accommodate about 5.3 holes per fu . A more detailed analysis of hole distribution is presented in Table I. The mean value of the probability of accommodating a hole on one atom is schematically presented in Fig. 8 by the thickness of the contour surrounding atoms of each group (chain, ladder-leg, ladder-rung).

The role of correlations is even more evident when analyzing hole and spin order along the chains in the paramagnetic DFT calculations and in the DFT including U and AF ordering. When correlation effects are switched-

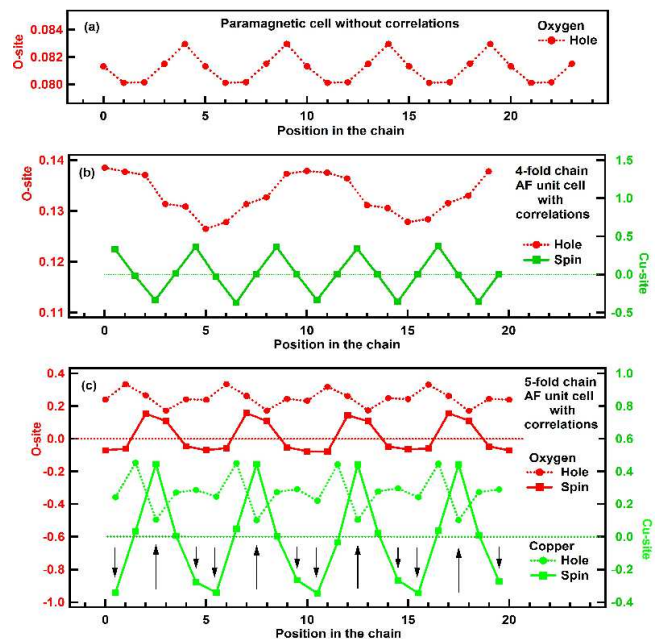


FIG. 7: (Color online) Chain site dependent hole (spin) density : (a) Chains have natural 5-fold hole periodicity in the paramagnetic cell without correlations ; (b) When the 4-fold chain spin periodicity is imposed, the 5-fold hole periodicity is destroyed ; (c) In the case of the 5-fold spin periodicity, the natural hole periodicity is preserved, on oxygen and as well on copper sites.

	Chain-	Ladder-			Sr-inter-layer
n	5.3	0.4			0.3
atom	Cu O	Cu	O(leg)	O(rung)	Sr
N_g	10 20	14	14	7	14
n_g	2.75 2.55	0.21	0.14	0.05	0.3

TABLE I: Calculated fraction (n) of 6 holes per fu residing in chain-, ladder- and in Sr-inter-layers of $\text{Sr}_{14}\text{Cu}_{24}\text{O}_{41}$; number of atoms in each group (N_g) ; distribution of holes between Cu- and O-sites in chains and ladders (n_g).

on the number of holes in the ladder is decreased by a factor of five. *Hole-depletion of ladders is thus a pure correlation effect.*

The distribution of more than 5 holes in chains and less than 1 in ladders is compatible not only with the AF unit cell with 5-fold chain periodicity, but also with the AF model with 4-fold chain periodicity.²⁷ But the latter model turns out to be irrelevant since in this case the NEXAFS calculations could not reproduce the experimental data (see Sect.III B). Moreover, the 4-fold chain-spin periodicity destroys the natural 5-fold hole ordering, while the 5-fold spin periodicity preserves it, as shown in Fig.7. We would like to stress once more that taking into account the proper long-range AF order is crucial to achieve a correct description of O K-edge NEXAFS

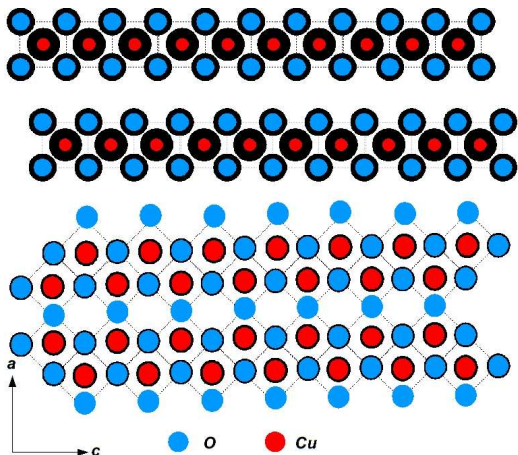


FIG. 8: (Color online) The thickness of the contour at O/Cu sites symbolizes the mean hole density per site in chains (upper panel) and ladders (lower panel) as determined by *ab-initio* calculations.

spectra.

It is worthwhile noting that our DOS is in good agreement with experiments as we find the occurrence of a strong -2 eV band with mixed chain/ladder contributions and large Cu-ladder weight, in accordance with Angle Resolved Photoemission Spectroscopy (ARPES) measurements.³⁴ Furthermore the two ladder-DOS structures at -0.25 eV and -0.1 eV have also been observed in a recent ARPES³⁵ experiment and were identified as the quasi-1D underlying Fermi surface.

Finally, the tendency of hole-depleting ladder-rungs found in our work, provides a satisfactory explanation for the 2D to 1D cross-over when the number of holes in the system is reduced, like in under-doped compounds³ or at low temperature where the less localized ladder sub-system suffers from the migration of holes to chains (back-transfer) as reported in the NMR.³⁶ On the fully doped side we suggest that the Ca doping has a twofold effect: it destroys long-range AF order in chains^{9,37,38} and reduces hole-depletion in ladders. Increased population of the rung sites reinforces the 2D character of the ladders. For sufficient Ca-induced ladder-doping the

CDW ground state is then suppressed in favor of the 2D superconductivity under pressure.^{1,39}

IV. CONCLUSION

In conclusion, our experimental NEXAFS spectra and first-principles theoretical modeling including the complete 316 atom AF unit cell, core-hole and correlation effects demonstrate that holes mainly reside on chains and thus ladders are hole-depleted. This finding resolves long standing controversial interpretations by several authors based on semi-empirical models. The analysis by Nücker et al.⁵ is in agreement with our findings based on an *ab-initio* approach. It is clear, however, that their arguments were based on a too limited description since correlations and long range AF behavior consisting of a 5-fold chain periodicity must be included to obtain the correct interpretation of the experimental spectra.

In ladders, majority of holes reside in leg sites, while only a tiny minority populates rung sites. Further experiments and calculations are under consideration to verify our suggestion that the small affinity of rung sites in the parent compound explains the 1D - 2D cross-over going from the under-doped to the fully doped side in the phase diagram of $(\text{La}, \text{Y}, \text{Sr}, \text{Ca})_{14}\text{Cu}_{24}\text{O}_{41}$.

Our work unambiguously answers the out-standing question of where the holes reside in $\text{Sr}_{14}\text{Cu}_{24}\text{O}_{41}$. This is crucial to understanding all phenomena occurring in the phase diagram of this family of compounds, ranging from charge-ordered antiferromagnetism to superconductivity and is a prerequisite to all investigations based on correlated models of spin ladder and chain compounds.²

V. ACKNOWLEDGMENTS

M. C. and C. G. acknowledge discussions with F. Mauri. Calculations were performed at the IDRIS superconducting center (project number 96053). S. T. acknowledges support from the Croatian Ministry of Science, Education and Sports under grant 035-0000000-2836.

* Electronic address: vita.ilakovac-casses@upmc.fr

¹ M. Uehara, T. Nagata, J. Akimitsu, H. Takahashi, N. Môri, K. Kinoshita, J. Phys. Soc. Jpn. **65**, 2764 (1996)

² T. Vuletić, B. Korin-Hamzić, T. Ivek, S. Tomić, B. Gorshunov, M. Dressel, J. Akimitsu, Phys. Rep. **428**, 169 (2006)

³ T. Ivek, T. Vuletić, B. Korin-Hamzić, O. Milat, S. Tomić, B. Gorshunov, M. Dressel, J. Akimitsu, Y. Sugiyama, C. Hess, and B. Büchner, Phys. Rev. B **78** 205105 (2008)

⁴ T. Osafune, N. Motoyama, H. Eisaki, and S. Uchida, Phys. Rev. Lett. **78**, 1980 (1997)

⁵ N. Nücker, M. Merz, C. A. Kuntscher, S. Gerhold, S. Schuppler, R. Neudert, M. S. Golden, J. Fink, D. Schild, S. Stadler, V. Chakarian, J. Freeland, Y. U. Idzerda, K. Conder, M. Uehara, T. Nagata, J. Goto, J. Akimitsu, N. Motoyama, H. Eisaki, S. Uchida, U. Ammerahl, A. Revcolevschi, Phys. Rev. B **62**, 14384 (2000)

⁶ E. Kabasawa, J. Nakamura, N. Yamada, K. Kuroki, H. Yamazaki, M. Watanabe, J. D. Denlinger, S. Shin, and R. C. C. Perera, J. Phys. Soc. Jpn. **77**, 034704 (2008)

⁷ E. Tafra, B. Korin-Hamzić, M. Basletić, A. Hamzić, M. Dressel and J. Akimitsu, Phys. Rev. B **78**, 155122 (2008)

- ⁸ M. Takigawa, N. Motoyama, H. Eisaki, S. Uchida, Phys. Rev. B **57**, 1124 (1998)
- ⁹ M. Matsuda, T. Yoshizawa, K. Kakurai, G. Shirane, Phys. Rev. B **59**, 1060 (1999)
- ¹⁰ R. S. Eccleston, M. Uehara, J. Akimitsu, H. Eisaki, N. Motoyama, and S. I. Uchida, Phys. Rev. Lett. **81**, 1702 (1998)
- ¹¹ L. P. Regnault, J. P. Boucher, H. Moudden, J. E. Lorenzo, A. Hiess, U. Ammerahl, G. Dhalenne, and A. Revcolevschi, Phys. Rev. B **59**, 1055 (1999)
- ¹² M. Troyer, H. Tsunetsugu, and D. Würtz, Phys. Rev. B **50**, 13515 (1994)
- ¹³ S. Notbohm, P. Ribeiro, B. Lake, D. A. Tennant, K. P. Schmidt, G. S. Uhrig, C. Hess, R. Klingeler, G. Behr, B. Büchner, M. Reehuis, R. I. Bewley, C. D. Frost, P. Manuel, and R. S. Eccleston, Phys. Rev. Lett. **98**, 027403 (2007)
- ¹⁴ J. Schlappa, T. Schmitt, F. Vernay, V. N. Strocov, V. Ilakovac, B. Thielemann, H. M. Ronnow, S. Vanishri, A. Piazzalunga, X. Wang, L. Braicovich, G. Ghiringhelli, C. Marin, J. Mesot, B. Delley, and L. Patthey, Phys. Rev. Lett. **103**, 047401 (2009)
- ¹⁵ P. Abbamonte, G. Blumberg, A. Rusydi, A. Gozar, P. G. Evans, T. Siegrist, L. Venema, H. Eisaki, E. D. Isaacs, and G. W. Sawatzky, Nature **431**, 1078 (2004)
- ¹⁶ A. Rusydi, M. Berciu, P. Abbamonte, S. Smadici, H. Eisaki, Y. Fujimaki, S. Uchida, M. Rübhausen, and G. A. Sawatzky, Phys. Rev. B **75**, 104510 (2007)
- ¹⁷ F. C. Zhang and T. M. Rice, Phys. Rev. B **37**, R3759 (1988)
- ¹⁸ M. Taillefumier, D. Cabaret, A.-M. Flank, and F. Mauri, Phys. Rev. B **66**, 195107 (2002)
- ¹⁹ C. Gougoussis, M. Calandra, A. Seitsonen, Ch. Brouder, A. Shukla, and F. Mauri, Phys. Rev. B **79**, 045118 (2009)
- ²⁰ C. Gougoussis, M. Calandra, A. P. Seitsonen, and F. Mauri, Phys. Rev. B **80**, 075102 (2009)
- ²¹ P. Gianozzi et al., J. Phys.: Condens. Matter **21**, 395502 (2009)
- ²² P. E. Blöchl, Phys. Rev. B **50**, 17953 (1994)
- ²³ V. I. Anisimov, F. Aryasetiawan, and A. I. Lichtenstein, J. Phys.: Condens. Matter **9**, 767 (1997)
- ²⁴ M. Cococcioni and S. de Gironcoli, Phys. Rev. B **71**, 035105 (2005)
- ²⁵ Y. Gotoh, I. Yamaguchi, Y. Takahashi, J. Akimoto, M. Goto, M. Onoda, H. Fujino, T. Nagata, and J. Akimitsu, Phys. Rev. B **68**, 224108 (2003)
- ²⁶ M. v. Zimmermann, J. Geck, S. Kiele, R. Klingeler, and B. Büchner, Phys. Rev. B **73**, 115121 (2006)
- ²⁷ D. E. Cox, T. Iglesias, K. Hirota, G. Shirane, M. Matsuda, N. Motoyama, H. Eisaki, and S. Uchida, Phys. Rev. B **57**, 10750 (1998)
- ²⁸ M. Arai and H. Tsunetsugu, Phys. Rev. B **56**, R4305 (1997)
- ²⁹ U. Schwingenschlögl and C. Schuster, Eur. Phys. J. B **55**, 43 (2007)
- ³⁰ C. Ma, H. X. Yang, L. J. Zeng, Y. Zhang, L. L. Wang, L. Chen, R. Xiong, J. Shi, and J. Q. Li, J. Phys.: Condens. Matter **21**, 215606 (2009)
- ³¹ N. Motoyama, T. Osafune, T. Kakeshita, H. Eisaki, S. Uchida, Phys. Rev. B **55**, R3386 (1997)
- ³² G. Blumberg, P. Littlewood, A. Gozar, B. S. Dennis, N. Motoyama, H. Eisaki, S. Uchida, Science **297**, 584 (2002)
- ³³ T. Vuletić, T. Ivek, B. Korin-Hamzić, S. Tomić, B. Gorshunov, P. Haas, M. Dressel, J. Akimitsu, T. Sasaki, and T. Nagata, Phys. Rev. B **71**, 012508 (2005)
- ³⁴ T. Takahashi, T. Yokoya, A. Ashihara, O. Akaki, H. Fujisawa, A. Chainani, M. Uehara, T. Nagata, J. Akimitsu, H. Tsunetsugu, Phys. Rev. B **56**, 7870 (1997)
- ³⁵ T. Yoshida, X. J. Zhou, Z. Hussain, Z.-X. Shen, A. Fujimori, H. Eisaki, and S. Uchida, Phys. Rev. B **80**, 052504 (2009)
- ³⁶ Y. Piskunov, D. Jérôme, P. Auban-Senzier, P. Wzietek, and A. Yakubovskiy, Phys. Rev. B **72**, 064512 (2005)
- ³⁷ T. Nagata, H. Fujino, J. Akimitsu, M. Nishi, K. Kakurai, S. Katano, M. Hiroi, M. Sera, N. Kobayashi, J. Phys. Soc. Jpn. **68**, 2206 (1999)
- ³⁸ M. Isobe, M. Onoda, T. Ohta, F. Izumi, K. Kimoto, E. Takayama-Muromachi, A. W. Hewat, K. Ohoyama, Phys. Rev. B **62**, 11667 (2000)
- ³⁹ T. Vuletić, B. Korin-Hamzić, S. Tomić, B. Gorshunov, P. Haas, T. Room, M. Dressel, J. Akimitsu, T. Sasaki, and T. Nagata, Phys. Rev. Lett. **90**, 257002 (2003)